

Preparation and Characterization of Co^{II}, Ni^{II}, and Zn^{II} Complexes of Sterically Demanding Hexaazamacrocyclic Dithiophenolates

Mathias Gressenbuch,^[a] Vasile Lozan,^[a] Gunther Steinfeld,^[b] and Berthold Kersting*^[a]

Keywords: Binding pockets / Macrocyclic ligands / Cobalt / Nickel / Zinc

N-Alkylated variants of a Robson-type 24-membered hexaazamacrocyclic dinucleating dithiophenolate ligand bearing ethyl and propyl groups have been prepared and their ligating properties towards the 3d elements Ni, Co and Zn have been examined. The new ligands support the formation of dinuclear complexes of the type $[(L^R)M_2(L')^+]^+$, i.e. $[(L^{Et})Ni_2(Cl)]^+$ (**7**), $[(L^{Pr})Ni_2(Cl)]^+$ (**8**), $[(L^{Et})Ni_2(OAc)]^+$ (**9**), $[(L^{Pr})Ni_2(OAc)]^+$ (**10**), $[(L^{Et})Ni_2(O_2COMe)]^+$ (**11**), $[(L^{Et})Ni_2(O_2COEt)]^+$ (**12**), $[(L^{Et})Zn_2(OAc)]^+$ (**14**), $[(L^{Et})Co_2(Cl)]^+$ (**17**), and $[(L^{Et})Co_2(OAc)]^+$ (**18**), the overall structures of which are very similar to the corresponding complexes of the parent permethylated ligand system. The use of the longer alkyl chains expands the binding pocket of the complexes to a more conical, "calixarene"-like cavity and has allowed for

the isolation of the trication $[(HL^{Et})Ni_2]^{3+}$ (**13**), which is an intermediate in the substitution reactions of **7**. Complex **13** reveals a new coordination mode of the supporting ligand with adjacent four- and five-coordinate nickel atoms. Its higher stability is presumably a consequence of the increased steric crowding imposed by the longer alkyl chains of $(L^{Et})^{2-}$. These results have thus demonstrated that these highly functionalized ligand systems allow for the stabilization of reactive intermediates. This information can now be used as a guide to further modulate the chemical reactivity of these compounds.

(© Wiley-VCH Verlag GmbH & Co. KGaA, 69451 Weinheim, Germany, 2005)

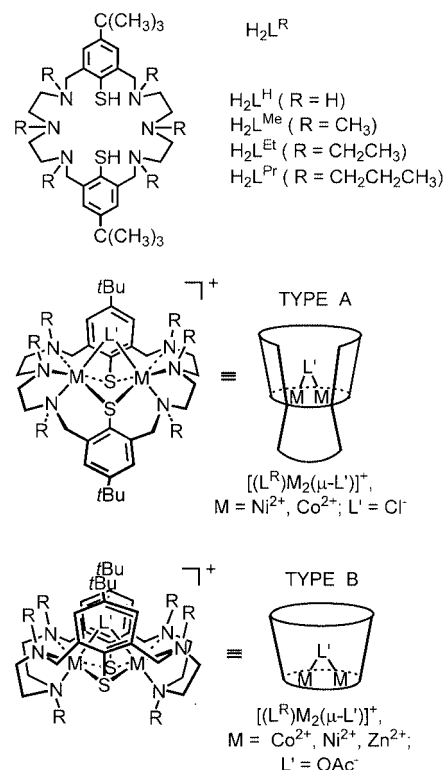
Introduction

Much effort is currently been invested in the design and development of supporting ligands for the construction of metal complexes with deep binding pockets.^[1] Several suitable ligand systems have already been reported, as for instance the calixarenes,^[2,3] the cyclodextrins^[4,5] and some highly functionalized chelate ligands.^[6,7] Recently, we reported that the Robson-type^[8] macrocycles H_2L^H and its permethylated derivative H_2L^{Me} (see Scheme 1) can also be employed for this purpose.^[9] Both ligands support the formation of $[(L^R)M_2(\mu-L')^+]^+$ complexes, whose ligand conformations are reminiscent of the "partial cone" and "cone" conformations of the calixarenes.

It has been observed that the binding pocket influences the coordination chemistry of the $[(L^R)M_2(\mu-L')^+]^+$ complexes significantly. For example, the substitution rates of the bridging coligands (L') are drastically increased.^[10] Likewise, it allows for the activation of small molecules such as carbon dioxide,^[11] and it can mediate the course of substrate transformations as seen in the highly diastereoselective *cis*-bromination of α,β -unsaturated carboxylate coligands.^[12]

[a] Institut für Anorganische Chemie, Universität Leipzig, Johannisallee 29, 04103 Leipzig, Germany
Fax: + 49-341-97-36199
E-Mail: b.kersting@uni-leipzig.de

[b] Institut für Anorganische und Analytische Chemie, Universität Freiburg, Albertstr. 21, 79104 Freiburg



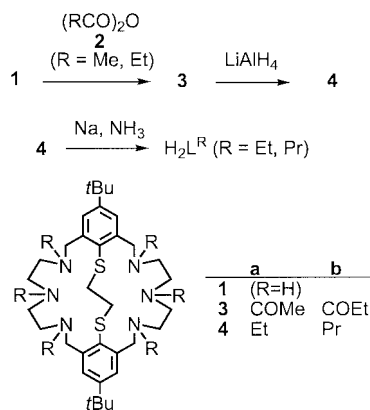
Scheme 1. Structure of the ligands (H_2L^R) and schematic representation of the structures of their corresponding metal complexes $[(L^R)M_2(\mu-L')^+]^+$. The cavity representation of the ligands $(L^R)^{2-}$ should not be confused with the one used for cyclodextrins.

These results prompted us to expand the binding pocket of this versatile ligand system by using alkyl groups larger than methyl and to investigate the effect of this modification on the ligating properties. In this paper, we describe the synthesis and characterization of *N*-alkylated variants of $\text{H}_2\text{L}^{\text{Me}}$ bearing ethyl and propyl groups in place of the methyl functions and report on their ligating properties towards the 3d elements Ni, Co and Zn (see Scheme 1 for abbreviations).

Results and Discussion

Ligand Synthesis

Two new derivatives of the parent hexaazamacrocyclic dithiophenolate $\text{H}_2\text{L}^{\text{H}}$ with ethyl and propyl substituents were prepared in order to probe the influence of ligand structural variations on metal ion complexation and metal complex structures. For the bulkier ethyl and propyl derivatives a reaction sequence similar to that used for the alkylation of triazacyclononane^[13] and cyclam^[14] was used. The syntheses began with the acylation of known amine **1**,^[15] with the anhydrides **2** (Scheme 2). The resulting amides **3** were then reduced with lithium aluminium hydride in refluxing THF solution to give the corresponding amines **4**. The thioether functions of the latter compounds were deprotected in the usual way^[16] with sodium in liquid ammonia to afford the desired ligands which could be readily isolated as hydrochloride salts $\text{H}_2\text{L}^{\text{R}}\cdot 6\text{HCl}$ ($\text{R} = \text{Et}, \text{Pr}$). All new compounds were characterized by elemental analysis, IR, ^1H and ^{13}C NMR spectroscopy. The hydrochloride salts of the ligands could not be obtained in analytically pure form. However, they were of sufficient purity for metal complex syntheses.



Scheme 2. Preparation of the ligands $\text{H}_2\text{L}^{\text{Et}}$ and $\text{H}_2\text{L}^{\text{Pr}}$.

Synthesis of Complexes

The synthesized compounds and their labels are collected in Table 1. Of these, the compounds $[(\text{L}^{\text{Me}})\text{Ni}^{\text{II}}_2(\mu\text{-Cl})]\text{ClO}_4$ (**5**· ClO_4) and $[(\text{L}^{\text{Me}})\text{Ni}^{\text{II}}_2(\mu\text{-OAc})]\text{ClO}_4$ (**6**· ClO_4) were reported previously.^[10,11] According to these procedures, the

macrocycles $\text{H}_2\text{L}^{\text{Et}}$ and $\text{H}_2\text{L}^{\text{Pr}}$ were allowed to react with $\text{NiCl}_2\cdot 6\text{H}_2\text{O}$ and triethylamine in 1:2:8 molar ratios in methanolic solution according to Equation (1). In the case of the ethylated derivative $\text{H}_2\text{L}^{\text{Et}}$, the complexation reaction was complete after stirring at ambient temperature for 3 d. Upon addition of LiClO_4 to the bright yellow solution, yellow microcrystals of $[(\text{L}^{\text{Et}})\text{Ni}^{\text{II}}_2(\mu\text{-Cl})]\text{ClO}_4$ (**7**· ClO_4) could be obtained in 82% yield. The propylated ligand $\text{H}_2\text{L}^{\text{Pr}}$ reacted similarly, generating the yellow species $[(\text{L}^{\text{Pr}})\text{Ni}^{\text{II}}_2(\mu\text{-Cl})]\text{ClO}_4$ (**8**· ClO_4), but stirring for 1 week was necessary to obtain it in comparable yields. In this respect, the two new ligands contrast the sterically less bulky ones which form dinuclear species more quickly. Characterization by elemental analysis, IR and UV/Vis spectroscopy {previously reported for $[(\text{L}^{\text{Me}})\text{Ni}^{\text{II}}_2(\mu\text{-Cl})]\text{ClO}_4$ (**5**· ClO_4)} are indicative of analogous bioctahedral structures of type A for these chloro-bridged compounds.

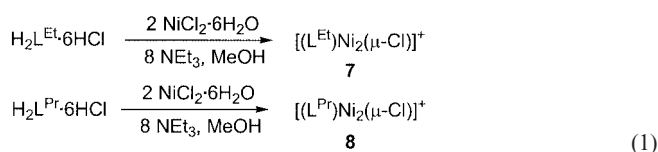
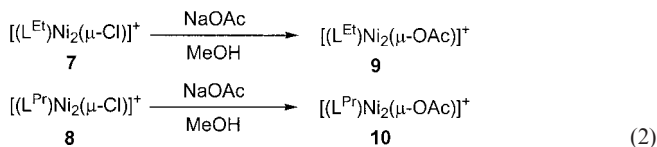


Table 1. Synthesized complexes, their labeling and selected structural data.^[a]

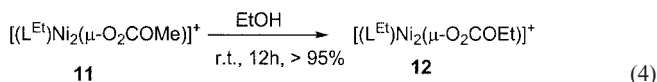
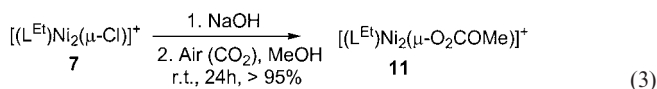
Compound	Structure	Ref.
	$[d(\text{M}\cdots\text{M})/\text{\AA}]$	
5	$[(\text{L}^{\text{Me}})\text{Ni}^{\text{II}}_2(\mu\text{-Cl})]^+$	A [3.201] ^[10]
6	$[(\text{L}^{\text{Me}})\text{Ni}^{\text{II}}_2(\mu\text{-OAc})]^+$	B [3.483] ^[11]
7	$[(\text{L}^{\text{Et}})\text{Ni}^{\text{II}}_2(\mu\text{-Cl})]^+$	A ^[b] this work
8	$[(\text{L}^{\text{Pr}})\text{Ni}^{\text{II}}_2(\mu\text{-Cl})]^+$	A ^[b] this work
9	$[(\text{L}^{\text{Et}})\text{Ni}^{\text{II}}_2(\mu\text{-OAc})]^+$	B ^[c] this work
10	$[(\text{L}^{\text{Pr}})\text{Ni}^{\text{II}}_2(\mu\text{-OAc})]^+$	B [3.513] this work
11	$[(\text{L}^{\text{Et}})\text{Ni}^{\text{II}}_2(\mu\text{-O}_2\text{COMe})]^+$	B ^[c] this work
12	$[(\text{L}^{\text{Et}})\text{Ni}^{\text{II}}_2(\mu\text{-O}_2\text{COEt})]^+$	B [3.520] this work
13	$[(\text{HL}^{\text{Et}})\text{Ni}^{\text{II}}_2]^{3+}$	[3.319] this work
14	$[(\text{L}^{\text{Et}})\text{Zn}^{\text{II}}_2(\mu\text{-OAc})]^+$	B [3.459] this work
15	$[(\text{L}^{\text{Me}})\text{Co}^{\text{II}}_2(\mu\text{-Cl})]^+$	A [3.180] ^[9b]
16	$[(\text{L}^{\text{Me}})\text{Co}^{\text{II}}_2(\mu\text{-OAc})]^+$	B [3.448] ^[9b]
17	$[(\text{L}^{\text{Et}})\text{Co}^{\text{II}}_2(\mu\text{-Cl})]^+$	A ^[b] this work
18	$[(\text{L}^{\text{Et}})\text{Co}^{\text{II}}_2(\mu\text{-OAc})]^+$	B [3.482] this work

[a] The complexes were isolated as ClO_4^- or BPh_4^- salts. [b] The experimentally determined structures of **5** and **15** suggest that complexes **7**, **8** and **17** adopt the form A. [c] The experimentally determined structures of **10** and **12** suggest that complexes **9** and **11** adopt the form B.

The bridging halide ions in complexes **7** and **8** proved quite labile. Thus, the reactions of the respective $[(\text{L})\text{Ni}_2(\mu\text{-Cl})]^+$ cations with sodium acetate proceeded smoothly and yielded green solutions, from which green crystals of $[(\text{L}^{\text{Et}})\text{Ni}_2(\mu\text{-OAc})]\text{ClO}_4$ (**9**· ClO_4) and $[(\text{L}^{\text{Pr}})\text{Ni}_2(\mu\text{-OAc})]\text{ClO}_4$ (**10**· ClO_4) were obtained in good yields [Equation (2)]. Later studies revealed that the same compounds can also be directly synthesized from the respective ligands and $\text{Ni}(\text{OAc})_2\cdot 6\text{H}_2\text{O}$.

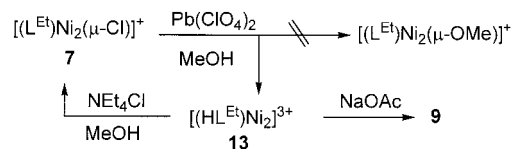


The methyl carbonate species **11** and its corresponding ethyl carbonate derivative **12** represent two further examples of nickel complexes of the ethylated macrocycle. Compound **11** was obtained by a carbonation reaction of the green μ -hydroxo species $[(L^{Et})Ni^{II}_2(\mu-OH)]^+$ (prepared in situ from **7** and sodium hydroxide; Equation (3)) and isolated as the pale-green perchlorate salt **11**·ClO₄ in 88% yield. The conversion of the methyl carbonate complex **11** into the ethyl carbonate species **12** was accomplished by a transesterification reaction with neat ethanol [Equation (4)]. Similar transformations were previously observed for the nickel complex **5** of the permethylated macrocycle. Thus, the rate of the substitution reactions and the ability to fix small molecules is not drastically altered by the longer alkyl chains.



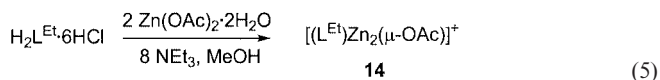
The compound $[(HL^{Et})Ni^{II}_2]^{3+}$ (**13**) formed rather unexpectedly during attempts to prepare a methanolato-bridged complex $[(L^{Et})Ni^{II}_2(\mu-Ome)]^+$ (Scheme 3). Instead of the anticipated compound the dark-green trication **13** was obtained. It could be isolated as the triperchlorate salt **13**·(ClO₄)₃ but only in low yield. This compound differs from the ones above in several respects. It bears no coligands, reveals a central N₂Ni(μ-S)₂NiN₃ core structure with adjacent four- and five-coordinate Ni^{II} ions and shows one protonated (non-coordinating) amine function (see below). It reacts readily with Et₄NCl to regenerate the parent complex **7**, and produces the acetato-bridged compound **9** upon addition of sodium acetate (Scheme 3). Recall that **7** is a type A species whereas **9** is of the kind B. The reaction in Equation (2) therefore involves a conformational change of the macrocycle from A to B. It can be shown that this requires an inversion of the configurations of the tertiary nitrogen donor atoms; however, this can only proceed by dissociation of the metal–nitrogen bonds. The crystal structure of **13** reveals such non-coordinating nitrogen donor atoms. Thus, **13** is presumably an intermediate in the above substitution reactions [e.g. Equation (2)]. All attempts to isolate the analogous compound of the permethylated macrocycle have failed.^[17] Therefore, the isolation of **13** can be traced back to the sterically more demanding ethyl functions. As we will show below, the use of H₂L^{Et} in place of

H₂L^{Me} results in restricted access to the two metal ions which are buried inside a sterically more encumbered cavity. This clearly shows that these highly functionalized macrocycles allow for the stabilization of reactive intermediates.

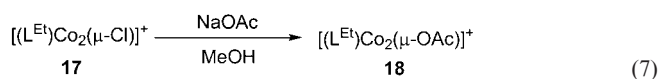
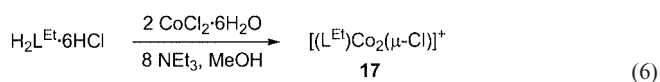


Scheme 3. Preparation and reactions of **13**.

To obtain some preliminary information on the solution structures, the synthesis of diamagnetic zinc complexes was devised next. The acetato-bridged dizinc complex **14** was obtained by the direct reaction of H₂L^{Et}·6HCl with Zn(OAc)₂·2H₂O and triethylamine in methanol [Equation (5)]. Attempts to prepare a chloro-bridged complex such as $[(L^{Et})Zn^{II}_2(\mu-Cl)]^+$ were unsuccessful.



The two Co^{II} complexes **17** and **18** represent the last two compounds of this study. These were prepared according to Equations (6) and (7). Both cations were isolated as their perchlorate salts in 83% and 74% yield, respectively. The structures of complexes $[(L^{Me})Co^{II}_2(\mu-Cl)]^+$ (**15**) and $[(L^{Me})Co^{II}_2(\mu-OAc)]^+$ (**16**) have previously been shown to be of type A and B, respectively.^[18] On the basis of spectroscopic similarities (vide infra), analogous structures are likely for the complexes supported by H₂L^{Et}. This is confirmed by an X-ray crystal structure determination of $[(L^{Et})Co^{II}_2(\mu-OAc)]BPh_4$ (**18**·BPh₄, see below).



All new complexes are stable in air both in solution and in the solid state. The perchlorate salts are very soluble in a range of common polar organic solvents (CH₃CN, EtOH, MeOH). The complexes with the longer alkyl chains also exhibit some solubility in apolar solvents such as cyclohexane or toluene. The new compounds gave satisfactory elemental analyses and were characterized by spectroscopic methods (IR, UV/Vis, ¹H and ¹³C NMR spectroscopy) and compounds **10**·ClO₄, **12**·BPh₄, **13**·(ClO₄)₃, **14**·ClO₄, and **18**·BPh₄ also by X-ray structure analysis.

Spectroscopic Characterization

Infrared Spectroscopy

The infrared spectra of all compounds display the bands expected for the macrocyclic ligands, counterions, carboxylate or alkyl carbonate coligands.^[19] Selected Infrared data are listed in Table 2. The ClO_4^- ion gives rise to a broad band at 1100 cm^{-1} which is normal for this counterion. The IR spectra of the acetato-bridged complexes **6**, **9**, **10**, **14**, **16**, and **18** are very similar. Each spectrum displays two strong bands around 1590 and 1430 cm^{-1} . These bands are associated with the asymmetric [$\nu_{\text{asym}}(\text{OAc}^-)$] and symmetric stretching modes [$\nu_{\text{sym}}(\text{OAc}^-)$] of the carboxylate coligands.^[20] The similarities to the IR spectrum of the dinickel complex **6** are indicative of $\mu_{1,3}$ -bridging acetate groups. The IR spectra of complexes **7**, **8**, **15**, and **17** lack these two bands, which is in good agreement with the formulation of the chloro-bridged $[(\text{L}^{\text{Mc}})\text{M}_2(\mu\text{-Cl})]^+$ cations. As can be seen in Table 2, the asymmetric and symmetric stretching modes of the alkyl carbonate complexes **11** and **12** are shifted to higher and lower frequencies, respectively, when compared with the corresponding values for the acetato-bridged compounds. This trend has also been observed for the carboxylate and alkyl carbonate complexes of the permethylated macrocycle.^[11] We finally note that the methyl and ethyl carbonate complexes can be easily distinguished by their IR spectra [e.g. by the frequency of the $\nu_{\text{sym}}(\text{O}_2\text{CR})$ stretching mode].

UV/Vis Spectroscopy

All new complexes were further characterized by UV/Vis spectroscopy. The electronic absorption spectra of the complexes were recorded in the $300\text{--}1600\text{ nm}$ range in acetonitrile solution. Selected spectroscopic data are reported in Table 2. The data for complexes **5**, **6**, **15**, and **16** have been reported previously and are included for comparative purposes.

The spectra of the nickel complexes are similar but not identical. Each compound displays two weak absorption bands. One appears in the $620\text{--}670\text{ nm}$ range, the other one

is observed between 1000 and 1180 nm . These absorptions can be attributed to the d-d transitions $\nu_2 [^3A_{2g}(\text{F}) \rightarrow ^3T_{1g}(\text{F})]$ and $\nu_1 [^3A_{2g}(\text{F}) \rightarrow ^3T_{2g}(\text{F})]$, respectively, of an octahedral nickel(II) (d^8) ion. For the chloro-bridged compounds the ν_1 absorption is split presumably due to lower symmetry. The higher energy features below 400 nm (not listed in Table 2) result from $\pi\text{-}\pi^*$ transitions within the $(\text{L}^{\text{R}})^{2-}$ ligands. The slight differences in the position of the d-d transitions indicate that each complex retains its integrity in solution. This is also supported by the NMR spectroscopic data described below for the zinc complex **14**.

As expected, the UV/Vis spectrum of the $[(\text{HL}^{\text{Et}})_2\text{Ni}^{\text{II}}]^{3+}$ trication **13** is different from the bioctahedral complexes above. The spectrum is dominated by an intense absorption band at 574 nm , which can be tentatively assigned to a d-d transition of the planar four-coordinate NiN_2S_2 chromophore. It is a typical value for complexes containing planar NiN_2S_2 units.^[21] This intense absorption presumably obscures the weaker d-d transition bands of the five-coordinate NiN_3S_2 fragment.^[22]

The electronic absorption spectra of the four cobalt(II) complexes are again very similar. Each compound reveals a weak band at ca. 1260 nm which can be readily assigned to the $^4T_{1g}(\text{F}) \rightarrow ^4T_{2g}$ transition of an octahedral high-spin cobalt(II) ion.^[23] Further absorption bands are observed in the $500\text{--}600\text{ nm}$ range. These bands are attributable to components of the parent octahedral ligand field transitions, $^4T_{1g}(\text{F}) \rightarrow ^4T_{1g}(\text{P})$ and $^4T_{1g}(\text{F}) \rightarrow ^4A_{2g}$, split by lower symmetry. The more intense band at ca. 450 nm most probably arises from a thiolate-to-cobalt(II) charge transfer (LMCT) transition and the feature at ca. 350 nm from a $\pi\text{-}\pi^*$ transition within the $(\text{L}^{\text{R}})^{2-}$ ligand. Again, these spectroscopic findings clearly show that the coligands remain attached to the cobalt ions in the solution state.

NMR Spectroscopy

The ^1H NMR spectrum of the acetato-bridged zinc complex **14** displays only one set of signals, indicative of a single isomer. The four aromatic protons (C^{Ar}) and the *tert*-butyl protons [$\text{C}(\text{CH}_3)_3$] appear as singlets, implying C_{2v} sym-

Table 2. Selected UV/Vis and IR spectroscopic data for compounds **5–18**.

Compound	$\lambda_{\text{max}}/\text{nm}$ ($\epsilon/\text{M}^{-1}\text{ cm}^{-1}$)	$\nu_{\text{as}}, \nu_{\text{s}} (\text{O}_2\text{CR})$
5	658 (41), 920 (59), 1002 (80)	—
6	649 (28), 1134 (55)	1588, 1426
7	659 (30), 930 (53), 1026 (76)	—
8	674 (26), 931 (54), 1023 (74)	—
9	660 (29), 1180 (79)	1589, 1426
10	662 (29), 1183 (77)	1593, 1428
11	668 (22), 1136 (84)	1638, 1330
12	668 (28), 1140 (79)	1637, 1316
13	574 (850), 1016 (50)	—
14	352 (2290)	1584, 1442
15	357 (1523), 468 (590), 545 (162), 571 sh (137), 1237 (23)	—
16	440 (467), 523 (170), 542 (121), 565 sh (64), 608 sh (21), 1262 (33)	1587, 1434
17	342 (2401), 470 (602), 548 (175), 578 sh (162), 1280 (28)	—
18	440 (610), 528 (204), 1288 (44)	1588, 1439

[a] The UV/Vis and IR spectra were recorded for the perchlorate salts.^[b] Spectra were recorded in CH_3CN solution at 295 K . Concentration of solutions were ca. $1.0 \times 10^{-3}\text{ M}$.

metry for the $[(L^{Et})Zn_2(\mu-OAc)]^+$ cation (i.e. structure type B). This is further supported by the fact that the $[(L^{Et})Zn_2]^{2+}$ fragment gives rise to only 13 ^{13}C signals (9 for the aliphatic and 4 for the aromatic carbon atoms). The appearance of the 1H NMR signals for the methyl protons of the bridging acetato coligand at $\delta = 0.85$ ppm is also worth mentioning. This signal is shifted to high field when compared with free sodium acetate ($\delta = 1.83$ ppm). This can be understood in terms of the ring current. As can be seen from Figure 3, the methyl protons of the acetate groups are positioned in the binding cavity of the $[(L^{Et})Zn_2]^{2+}$ fragment slightly above the center of the two phenyl rings in the shielding region. Similar findings have been observed for the $[(L^{Me})Zn^{II}(\mu-OAc)]^+$ cation.^[24] In summary, the spectroscopic data have clearly established that all complexes exist as discrete and stable species with similar “cone”- and “partial-cone”-like conformations of the macrocycles. Thus, with the exception of complex **13**, the ligating properties of the new ligands are not very different from the parent $(L^{Me})^{2-}$ and $(L^H)^{2-}$ ligands.

X-ray Crystallography

The formulations of the new compounds were further confirmed by X-ray diffraction studies. Single crystals of X-ray quality were obtained for the perchlorate salts of **10**, **13**, and **14** and for the tetraphenylborate salts of **12** and **18**. Selected crystallographic data are listed in Table 4. The molecular structures of the complexes are displayed in Figures 1, 2, 3, 4 and 5, and selected bond lengths and angles are given in Table 3.

Description of the Structures of the Biocuboctahedral $[(L^R)-M_2(\mu-O_2CR)]^+$ Complexes

The structures of the biocuboctahedral species **10**, **12**, **14**, and **18** will be discussed first. A common labeling scheme for the $[(L^{Me})M_2]^{2+}$ fragments has been used to facilitate structural comparisons. The structure of the cation $[(L^{Me})Ni_2^{II}(\mu-OAc)]^+$ (**6**) has been reported previously, and its metrical parameters are also given for comparison.

Structure of the $[(L^R)M_2]^{2+}$ Fragment

It is appropriate to describe the structures of the $[(L^R)-M_2]^{2+}$ fragments first. The macrocycles adopt the conformation of type B, previously reported for the acetato-bridged complex **6** (Scheme 1).^[11] In each case, the two metal ions are coordinated in a square-pyramidal fashion by the two *fac*-N₃(μ-S)₂ donor sets of the doubly deprotonated macrocycles. The coordination of the exogenous coligands generates distorted octahedral environments for the metal ions. The metrical parameters of the central N₃M(μ-S)₂(μ-O₂CR)MN₃ cores are very similar (see Table 3). The diethylenetriamine units are *fac*-coordinated with one larger and two smaller N–M–N bond angles, which is most commonly observed in complexes with this tridentate unit.^[25] Likewise, the M–N bonds involving the four benzylic nitrogen donors are invariably longer (by ca. 0.1 Å) than the ones comprising the central nitrogen atoms of the linking diethylenetri-



Figure 1. Two perspective side views of the structure of the dinickel complex **10** with thermal ellipsoids drawn at the 50% probability level. Hydrogen atoms are omitted for reasons of clarity.

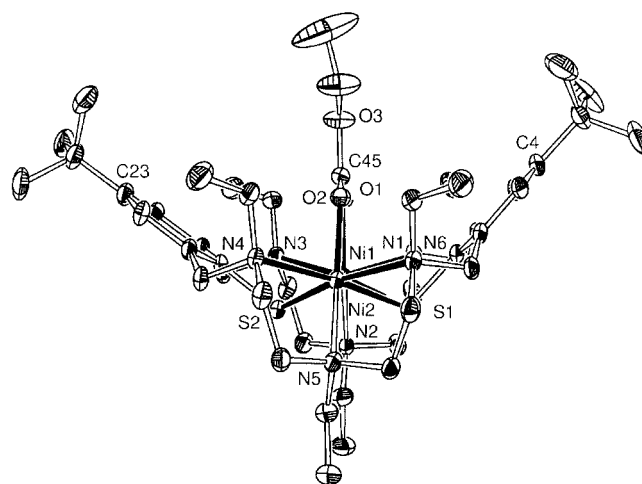


Figure 2. Structure of the dinickel complex **12** with thermal ellipsoids drawn at the 50% probability level. Hydrogen atoms are omitted for reasons of clarity.

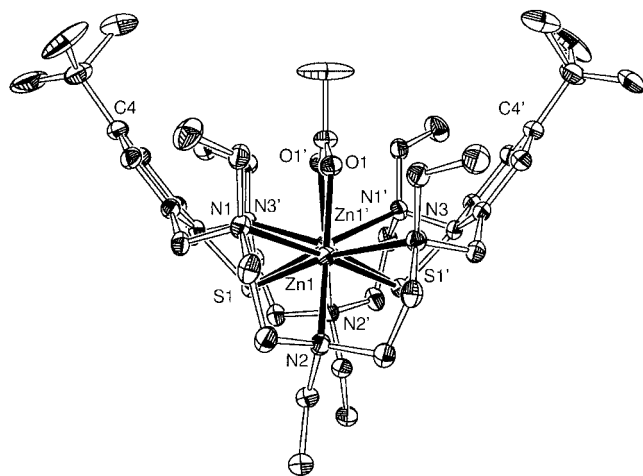


Figure 3. Structure of the dizinc complex **14** with thermal ellipsoids drawn at the 50% probability level. Only one orientation of the disordered *tert*-butyl group is displayed. Hydrogen atoms are omitted for reasons of clarity. Symmetry code used to generate equivalent atoms: $1 - x, y, 0.5 - z$ ($'$).

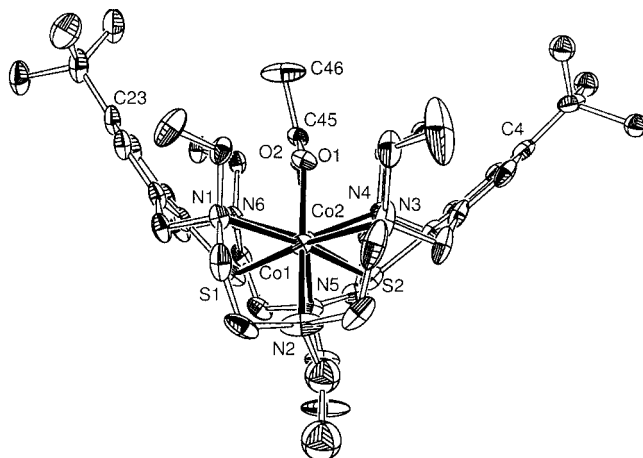


Figure 4. Structure of the dicobalt complex **18** with thermal ellipsoids drawn at the 50% probability level. Hydrogen atoms are omitted for reasons of clarity.

amine units. This is also normal for carboxylato-bridged structures of this ligand system [e.g. $[(L^{\text{Me}})M_2(\mu\text{-OAc})]^+$, $M = \text{Co}^{\text{II}}$, Ni^{II} , and Zn^{II}]. Hence, the differences in the metal–nitrogen bond lengths are due to steric constraints of the macrocycles.

Cavity Dimensions

As can be seen from Scheme 4, the four alkyl residues on the four benzylic nitrogen atoms align with the two phenyl rings. Thus, upon going from the methylated derivative to the *N*-propylated macrocycle the binding pocket of the $[(L^{\text{R}})M_2]^{2+}$ fragment expands to a sterically more encumbered, conical, calixarene-like cavity as schematically illustrated in Scheme 4.

The dimensions of the binding cavities of the $[(L^{\text{Me}})M_2]^{2+}$ fragments can be described by the intramolecular distances between the two opposing aryl ring carbon atoms bearing the *tert*-butyl groups [e.g. the diameter of the

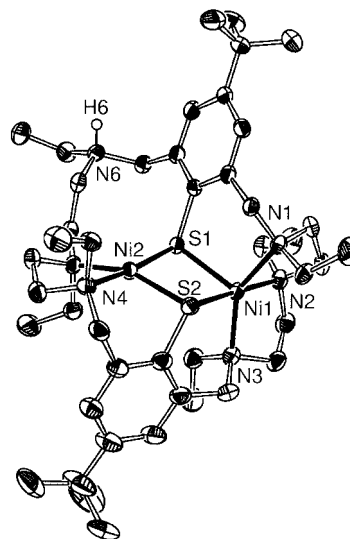
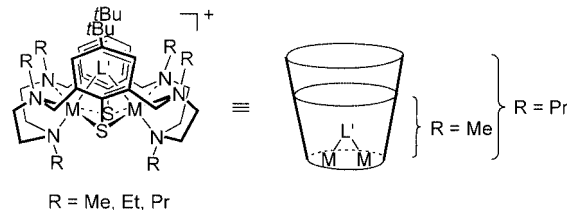


Figure 5. Structure of the dinickel complex **13** with thermal ellipsoids drawn at the 30% probability level. Only one orientation of the disordered *tert*-butyl and the *N*-propyl group is displayed. Selected bond lengths [Å] and angles [°]: Ni(1)···Ni(2) 3.319; Ni(1)–N(1) 2.051(3), Ni(1)–N(2) 2.138(3), Ni(1)–N(3) 2.060(3), Ni(1)–S(1) 2.2911(11), Ni(1)–S(2) 2.4065(13), Ni(2)–N(4) 1.991(3), Ni(2)–N(5) 1.997(3), Ni(2)–S(1) 2.2140(13), Ni(2)–S(2) 2.2129(12); N(5)–Ni(2)–S(2) 157.83(10), N(4)–Ni(2)–S(1) 171.76(10), N(2)–Ni(1)–S(2) 176.86(9), N(1)–Ni(1)–S(1) 100.57(9), N(3)–Ni(1)–S(1) 113.77(10), N(1)–Ni(1)–N(3) 145.55(12).



Scheme 4. Schematic representation of the expansion of the binding pocket of the $[(L^{\text{R}})M_2(L')^+]$ complexes upon going from the methylated ($R = \text{Me}$) to the propylated ligand system ($R = \text{Pr}$).

pocket entrance, see for example, $\text{C}(4) \cdots \text{C}(26)$ in **10**). The values range from 9.265 to 9.891 Å (Table 3). Two trends are apparent. Firstly, the diameter increases with increasing length of the *N*-alkyl residues (e.g. compare **6** with **10**). Secondly, the distances increase with increasing steric bulk of the coligand with this latter trend being the more important one (e.g. compare **10** with **12**). This is indicative of intramolecular steric repulsions between the residues of the bowl-shaped hosts and their guests.

Binding Mode of the Coligands

As expected, the acetate and ethyl carbonate coligands bind to the $[(L^{\text{Me}})M_2]^{2+}$ fragment as bidentate $\mu_{1,3}$ -bridges. Consequently, the $M \cdots M$ separations are almost equidistant in these three compounds [average value is 3.491(1) Å]. The average metal–ligand bond lengths show no unusual features and compare well with those in **6**.

Table 3. Selected bond lengths and angles of complexes **6**, **10**, **12**, **14** and **18**.

	6	10	12	14	18
M(1)–O(1)	1.998(2)	1.990(6)	2.020(3)	2.021(3)	1.993(3)
M(1)–N(1)	2.281(2)	2.321(7)	2.293(4)	2.362(3)	2.292(4)
M(1)–N(2)	2.152(2)	2.158(6)	2.156(4)	2.193(3)	2.212(4)
M(1)–N(3)	2.251(2)	2.238(9)	2.291(4)	2.418(3)	2.387(4)
M(1)–S(1)	2.493(1)	2.517(3)	2.494(1)	2.565(1)	2.495(2)
M(1)–S(2)	2.448(1)	2.423(2)	2.441(1)	2.535(1) (S1') ^[b]	2.502(2)
M(2)–O(2)	2.008(2)	1.985(5)	2.030(3)	2.021(3) (Zn1'–O1') ^[b]	2.004(3)
M(2)–N(4)	2.244(2)	2.247(6)	2.253(4)	2.362(3) (Zn1'–N1') ^[b]	2.313(4)
M(2)–N(5)	2.158(2)	2.174(6)	2.160(4)	2.193(3) (Zn1'–N2') ^[b]	2.191(6)
M(2)–N(6)	2.295(2)	2.334(7)	2.340(4)	2.418(3) (Zn1'–N3') ^[b]	2.312(5)
M(2)–S(1)	2.493(1)	2.507(2)	2.475(1)	2.565(1) (Zn1'–S1') ^[b]	2.492(1)
M(2)–S(2)	2.451(1)	2.423(3)	2.430(1)	2.535(1) (Zn1'–S1') ^[b]	2.538(2)
M–O	2.003(2)	1.988(6)	2.025(3)	2.021(3)	1.999(3)
M–N ^[a]	2.230(2)	2.245(7)	2.248(4)	2.324(3)	2.285(5)
M–S ^[a]	2.471(1)	2.468(3)	2.460(1)	2.550(3)	2.507(2)
M···M	3.483(1)	3.513(1)	3.520(1)	3.459(1) (Zn1–Zn1') ^[b]	3.482(1)
C(4)···C(20)	9.306	9.622 ^[d]	9.891 ^[e]	9.265 (C4–C4') ^[b]	9.563 ^[e]
S(1)–M(1)–S(2)	79.49(4)	77.94(8)	78.26(5)	82.20(5) (S1–Zn1–S1')	80.17(6)
S(1)–M(2)–S(2)	79.45(3)	78.11(8)	78.83(5)	82.20(5) (S1–Zn1'–S1')	79.55(5)
O(1)–M(1)–N(2)	163.89(7)	162.9(2)	164.81(14)	159.43(11)	158.40(15)
N(1)–M(1)–S(2)	170.28(5)	167.4(2)	168.21(11)	172.35(8) (N1–Zn1–S1')	169.98(10)
N(3)–M(1)–S(1)	170.09(5)	168.1(2)	168.31(10)	168.60(8)	168.51(10)
O(2)–M(2)–N(5)	163.84(7)	160.9(2)	164.90(14)	159.4(1) (O1'–Zn1'–N2')	159.7(2)
N(4)–M(2)–S(1)	170.86(5)	168.2(2)	169.16(10)	172.35(8) (N3'–Zn1'–S1')	169.74(11)
N(6)–M(2)–S(2)	169.28(5)	167.68(16)	168.08(10)	168.60(8) (N1'–Zn1'–N2')	168.47(12)
Ph/Ph ^[c]	80.8	88.1	95.2	76.0	83.8

[a] Average values. [b] Symmetry code used to generate equivalent atoms: 1 – x, +y, 0.5 – z ('). [c] Angle between the normals of the planes of the two aryl rings. [d] C(4)···C(26). [e] C(4)···C(23).

Description of the Crystal Structure of [(HL^{Et})Ni₂](ClO₄)₃·3MeOH·H₂O [13·(ClO₄)₃·3MeOH·H₂O]

This salt crystallizes in the triclinic space group $P\bar{1}$. The structure revealed the presence of discrete dinuclear [(HL^{Et})Ni₂]³⁺ trications, perchlorate anions, and methanol and water molecules of solvent of crystallization. As can be seen in Figure 5, this complex bears no coligands and features two differently coordinated nickel atoms. One nickel atom is coordinated in a distorted planar fashion by two *cis*-oriented nitrogen atoms and two bridging thiophenolate sulfur atoms. The other nickel ion is five-coordinate. The protonated amine donor N(6) is out of range of bonding interactions with the metal atoms and points away from them.

The coordination geometry of the four-coordinate nickel ion is significantly distorted from square-planar towards tetrahedral, as indicated by an N–Ni–N/S–Ni–S dihedral angle of 23.80(2)° (mean deviation from plane 0.238 Å). This is a rather large distortion from planarity. Other nickel complexes with N₂S₂ coordination environments are more rigorously square-planar, the tetrahedral twists from the NiN₂S₂ planes not exceeding 15°.^[26,27]

The coordination environment around the five-coordinate nickel atom is distorted trigonal-bipyramidal with S(1), N(1) and N(3) occupying the equatorial and S(2) and N(2) the axial positions. The angles in the equatorial plane deviate by as much as 25.6° [N(1)–Ni(1)–N(3)] from the ideal values of a perfect trigonal bipyramid. The average Ni–N and Ni–S distances of 2.083 and 2.349 Å are shorter than in the above bioctahedral species but compare well with those reported for [Ni^{II}(terpy)(S-2,4,6-(*i*Pr)₃C₆H₂)₂] (terpy =

2,2',2''-terpyridine; Ni–N 2.057 Å, Ni–S 2.303 Å)^[28] and other trigonal-bipyramidal Ni^{II}N₃S₂ complexes.^[29] The metal–ligand bonds involving the equatorial donor atoms are shorter than the ones comprising the axial ones; an exactly analogous situation is found in the terpy complexes. As a consequence of the shorter metal–ligand bonds, the metal···metal separation is smaller at 3.319 Å. Finally, it should be noted that the two nickel(II) ions are almost completely surrounded by the apolar *N*-ethyl substituents from the macrocycle. This steric crowding about the coordinatively unsaturated dinickel site might explain its higher stability {relative to the very unstable [(HL^{Me})Ni₂]³⁺ trication of the permethylated macrocycle}.

Summary and Conclusion

The following are the main findings of this investigation. a) *N*-Alkylated variants of H₂L^{Me} bearing ethyl and propyl groups in place of the methyl functions can be readily prepared by acylation of the parent hexamine–dithioether compound **1** followed by reduction of the amide and thioether functions. b) The new ligands support the formation of dinuclear complexes of the type [(L^R)M₂(μ-L')] with a bowl-shaped structure. c) The binding pocket of the complexes expands to a more conical, “calixarene”-like cavity upon going from the permethylated to the perpropylated ligand system. d) The rate of the substitution reactions and the ability to fix small molecules is not drastically altered by the longer alkyl chains. e) Finally, it has been demonstrated that these highly functionalized ligand systems allow

for the stabilization of reactive intermediates. These findings can now be used as a guide to further modulate the chemical reactivity of these compounds.

Experimental Section

Materials and Methods: Compound **1** was prepared as described in the literature.^[9] All syntheses were carried out under argon. Melting points were determined in open glass capillaries and are uncorrected. NMR spectra were recorded with a Bruker AVANCE DPX-200 spectrometer at 300 K. Chemical shifts refer to solvent signals. Infrared spectra were recorded with a Bruker VECTOR 22 FT-IR spectrometer and electronic absorption spectra with a Jasco V-570 UV/VIS/NIR spectrometer. Elemental analyses were carried out with a VARIO EL elemental analyzer. **CAUTION:** Perchlorate salts are potentially explosive and should therefore be prepared only in small quantities and handled with appropriate care!

Compound 3a: A solution of **1** (9.44 g, 15.4 mmol) in acetic anhydride (90 mL) was stirred at 50 °C for 6 h. After the solvent was distilled off at reduced pressure, the residue was taken up in aqueous potassium hydroxide solution (3 M, 100 mL) and dichloromethane (100 mL). The layers were separated and the aqueous phase was extracted with dichloromethane (3 × 50 mL). The combined organic layers were washed with water (50 mL) and dried with anhydrous sodium sulfate. Evaporation of the solvent gave **3a** as a white solid (13.1 g, 98%). M.p. 236 °C. This material was used in the next step without further purification. ¹H NMR (200 MHz, CDCl₃): δ = 1.06–1.26 [m, 18 H, ArC(CH₃)₃], 1.94–2.23 (m, 18 H, NCOCH₃), 2.82–3.35 (m, 20 H, NCH₂CH₂ and SCH₂), 4.47–4.74 (m, 8 H, ArCH₂), 6.91–7.10 (m, 4 H, ArH) ppm. IR (KBr): ν̄ = 3456 m, 2963 s, 2871 w, 1652 vs. ν(CO), 1559 vw, 1474 m, 1418 s, 1363 m, 1313 vw, 1238 w, 1195 w, 1131 vw, 1094 vw, 1062 vw, 1035 vw, 988 vw, 950 vw, 878 vw, 603 w cm⁻¹. C₄₆H₆₈N₆O₆S₂·CH₃CO₂H (865.19 + 60.05): calcd. C 62.31, H 7.99, N 9.52, S 7.26; found C 62.33, H 8.79, N 9.23, S 6.66.

Compound 4a: A solution of **3a** (8.65 g, 10.0 mmol) in tetrahydrofuran (50 mL) was added dropwise to a suspension of lithium aluminium hydride (4.55 g, 120 mmol) in tetrahydrofuran (200 mL). The reaction mixture was refluxed for 12 h. To the hot reaction mixture was added water (10 mL) in small portions followed by 3 M aqueous potassium hydroxide solution (30 mL). Care should be taken during this step because of the violent reaction. The reaction mixture was refluxed for an additional hour to ensure complete hydrolysis of the aluminum salts. After cooling to room temperature, the organic layer was decanted from a white residue. This residue was extracted with boiling tetrahydrofuran (3 × 100 mL). The combined organic layers were dried with anhydrous sodium sulfate. Evaporation of the solvent gave the title compound as a yellowish oil which was used in the next step without further purification (6.80 g, 87%). ¹H NMR (CDCl₃, 200 MHz): δ = 0.85–1.00 (m, 18 H, NCH₂CH₃), 1.23 [s, 18 H, ArC(CH₃)₃], 2.29–2.55 (m, 28 H, NCH₂CH₃ and NCH₂CH₂N), 2.70 (s, 4 H, SCH₂), 3.62 (s, 8 H, ArCH₂N), 7.41 (s, 4 H, ArH) ppm. ¹³C{¹H} NMR (50 MHz, CDCl₃): δ = 13.6, 13.8 (CH₃), 32.5 [ArC(CH₃)₃], 35.8 [ArC(CH₃)₃], 37.0 (ArSCH₂), 49.0 (CH₂), 51.0 (CH₂), 52.3 (CH₂), 53.0 (CH₂), 58.7 (CH₂), 125.8 (CH), 129.1 (C^{Ar}), 145.0 (C^{Ar}), 152.1 (C^{Ar}) ppm. IR (Nujol): ν̄ = 3417 m, 2964 vs, 2869 s, 2809 s, 2354 vw, 2327 vw, 1730 vw, 1713 vw, 1691 vw, 1659 vw, 1642 vw, 1631 vw, 1600 w, 1555 vw, 1513 vw, 1463 m, 1383 m, 1363 m, 1292 w, 1262 s, 1223 w, 1173 w, 1096 s, 1073 s, 865 vw, 802 s, 710 vw, 663 vw cm⁻¹.

Compound H₂L^{Et}·6HCl: To a solution of sodium (3.45 g, 150.0 mmol) in liquid ammonia (150 cm³) was added a solution of compound **4a** (3.91 g, 5.00 mmol) in tetrahydrofuran (50 cm³) dropwise at –78 °C. The resulting blue reaction mixture was stirred at –78 °C for one additional hour to ensure complete deprotection of the macrocycle. Solid ammonium chloride was added in small portions at –78 °C to destroy excess reducing agent. The resulting colourless suspension was allowed to warm to room temperature. After 12 h, the remaining solvent was distilled off at reduced pressure. The residue was taken up in water (50 mL) and the pH of the suspension adjusted to ca. 1 to give a pale-yellow solution of H₂L^{Et} as the hexahydrochloride salt. To remove the inorganic salts, the solution was concentrated in vacuo to a volume of about 20 mL. Methanol (ca. 60 mL) was then added and the resulting solution was filtered from NaCl and NH₄Cl. The latter two steps were repeated several times in this order, until no more salts precipitated upon addition of MeOH. A 100-mL portion of ethanol was then added. Upon standing for 1–2 h, the product precipitated as a pale-yellow solid (2.82 g, 58%). ¹H NMR (200 MHz, D₂O): δ = 1.29 [s, 18 H, ArC(CH₃)₃], 1.39 (m, 18 H, CH₂CH₃), 3.33 (m, 12 H, CH₂CH₃), 3.75–3.90 [m, 16 H, N(CH₂CH₂)₂], 4.59 (s br, 8 H, ArCH₂N), 7.56 (s, 4 H, ArH) ppm. ¹³C{¹H} NMR (50 MHz, D₂O): δ = 9.09 (CH₃), 9.21 (CH₃), 31.49 [ArC(CH₃)₃], 34.90 [ArC(CH₃)₃], 47.41 (CH₂), 48.73 (CH₂), 50.19 (CH₂), 50.39 (CH₂), 59.44 (CH₂), 131.74 (CH), 132.00 (C^{Ar}), 147.00 (C^{Ar}), 149.00 (C^{Ar}) ppm. This compound was pure enough for the preparation of the metal complexes. IR (KBr): ν̄ = 3407 vs, 2962 vs, 2624 vs, 1690 s, 1630 m, 1451 vs, 1400 vs, 1231 m, 1161 s, 1031 s, 898 vs, 801 vs, 565 vs cm⁻¹.

Compound 3b: The preparation of this compound was analogous to that of **3a**, except that propionic anhydride was used instead of acetic anhydride. **3b** was obtained as a white solid (8.92 g, 94%). M.p. 170–176 °C. This product was used in the next step without further purification. ¹H NMR (200 MHz, CDCl₃): δ = 1.17 (m, 18 H, NCOCH₂CH₃), 1.25–1.36 [m, 18 H, ArC(CH₃)₃], 2.70 (m, 12 H, NCOCH₂CH₃), 3.06–3.68 [m, 20 H, N(CH₂CH₂N)₂ + ArSCH₂], 4.90 (s, 8 H, ArCH₂N), 7.00–7.06 (m, 4 H, ArH) ppm. IR (KBr): ν̄ = 3441 w, 2967 m, 2939 m, 2876 w, 1724 vw, 1648 vs, 1563 vw, 1468 s, 1421 s, 1378 w, 1364 w, 1198 m, 1184 m, 1120 vw, 1079 w, 1052 w, 970 vw, 879 vw, 815 vw, 726 vw, 683 vw, 573 vw, 535 vw cm⁻¹. C₅₂H₈₀N₆O₆S₂ (949.36): calcd. C 65.79, H 8.49, N 8.85, S 6.76; found C 65.02, H 8.52, N 8.28, S 6.16.

Compound 4b: The preparation of this compound was analogous to **3b**. Compound **4b** was obtained as a yellowish oil which crystallized on standing. Recrystallization from ethanol gave 5.02 g (58%) of analytically pure material. M.p. 128 °C. ¹H NMR (CDCl₃, 200 MHz): δ = 0.77 (t, ³J = 7.2 Hz, 18 H, NCH₂CH₂CH₃), 1.23 [s, 18 H, ArC(CH₃)₃], 1.14–1.40 (m, 12 H, NCH₂CH₂CH₃), 2.26 (t, ³J = 7.2 Hz, 12 H, NCH₂CH₂CH₃), 2.48 (s, 16 H, NCH₂CH₂N), 2.63 (s, 4 H, ArSCH₂), 3.60 (s, 8 H, ArCH₂N), 7.45 (s, 4 H, ArH) ppm. ¹³C{¹H} NMR (CDCl₃, 75 MHz): δ = 12.3 (NCH₂CH₂CH₃), 21.2 (NCH₂CH₂CH₃), 21.6 (NCH₂CH₂CH₃), 31.8 [ArC(CH₃)₃], 35.2 [ArC(CH₃)₃], 35.7 (ArSCH₂), 51.5 (CH₂), 52.4 (CH₂), 56.1 (CH₂), 58.2 (CH₂), 59.2 (CH₂), 124.7 (CH), 127.7 (C^{Ar}), 144.2 (C^{Ar}), 151.4 (C^{Ar}) ppm. IR (KBr): ν̄ = 2958 s, 2933 s, 2870 m, 2817 m, 1460 m, 1404 w, 1380 w, 1361 w, 1079 m, 893 w, 647 w cm⁻¹. C₅₂H₉₂N₆S₂ (865.46): C 72.16, H 10.71, N 9.71, S 7.41; found C 71.92, H 10.86, N 9.60, S 7.30.

Compound H₂L^{Pr}·6HCl: The preparation of this compound was analogous to H₂L^{Et}·6HCl, except that **4b** (4.32 g, 5.00 mmol) was used as the starting material. The hydrochloride was obtained as a pale-yellow solid (3.33 g, 63%). ¹H NMR (200 MHz, D₂O): δ =

0.71 (t, ³J = 7.2 Hz, 18 H, NCH₂CH₂CH₃), 1.04 [s, 18 H, C(CH₃)₃], 1.60–1.35 (m, 12 H, NCH₂CH₂CH₃), 2.87 (m, 12 H, NCH₂CH₂CH₃), 3.44 (m, 16 H, NCH₂CH₂N), 4.30 (s, 8 H, ArCH₂N), 7.25 (s, 4 H, ArH) ppm. ¹³C{¹H} NMR (50 MHz, D₂O): δ = 10.4 (CH₃), 17.2 (CH₂), 17.4 (CH₂), 30.7 [ArC(CH₃)₃], 34.8 [ArC(CH₃)₃], 35.5 (CH₂), 47.3 (CH₂), 48.7 (CH₂), 56.0 (CH₂), 59.6 (CH₂), 61.9 (CH₂), 131.1 (CH), 134.3 (C^{Ar}), 147.9 (C^{Ar}), 158.4 (C^{Ar}) ppm. IR (KBr): $\tilde{\nu}$ = 3427 w, 2967 vw, 2878 w v(CH), 2465 w, 1629 s v(CO), 1471 w, 1384 m, 1364 m, 1300 s, 1200 m, 1150 m, 1051 s, 996 s, 967 s, 806 vs, 755 vs, 601 vs cm⁻¹. This compound was pure enough for the preparation of the metal complexes.

[(L^{Et})Ni₂(Cl)]ClO₄ (7-ClO₄): To a suspension of H₂L^{Et}·6HCl (974 mg, 1.00 mmol) in methanol (40 mL) was added a solution of NiCl₂·6H₂O (475 mg, 2.00 mmol) in methanol (2 mL). A solution of Et₃N (810 mg, 8.00 mmol) in methanol (2 mL) was then added to give a dark red solution. After stirring at room temperature for 3 d, the product was precipitated by the addition of solid LiClO₄·3H₂O (2.50 g, 15.6 mmol). The yellow microcrystalline solid was isolated by filtration, washed with 5 mL of cold ethanol and 5 mL of ether, and dried in vacuo. This material was recrystallized once from a few milliliters of acetonitrile. Yield: 824 mg (82%). M.p. 305 °C (decomp.). IR (KBr): $\tilde{\nu}$ = 3445 m, 2961 m, 2894 w, 2361 vw, 1631 w, 1460 m, 1381 w, 1100 vs v(ClO₄⁻), 912 w, 884 w, 778 w, 733 w, 627 m cm⁻¹. UV/Vis (CH₃CN): λ_{\max} (ε) = 384 (2070), 480 sh (430), 659 (30), 930 (53), 1026 nm (76 M⁻¹ cm⁻¹). C₄₄H₇₆Cl₂N₆Ni₂O₄S₂ (1005.53): calcd. C 52.56, H 7.62, N 8.36, S 6.38; found C 52.40, H 7.47, N 8.42, S 6.49.

[(L^{Pr})Ni₂(Cl)]ClO₄ (8-ClO₄): The preparation of this compound was similar to that of 7-ClO₄, except that the reaction mixture was stirred for 1 week. The compound was obtained as yellow microcrystals and purified by recrystallization from acetonitrile. Yield: 37%. M.p. 274 °C (decomp.). IR (KBr): $\tilde{\nu}$ = 3435 vs, 2964 vs, 2874 s, 2741 vw, 2665 vw, 2381 vw, 2179 vw, 2061 s, 1732 vw, 1630 s, 1607 s, 1464 s, 1365 m, 1328 vw, 1261 w, 1233 w, 1108 vs, 926 w, 912 w, 882 w, 805 m, 751 w, 629 s, 559 m cm⁻¹. UV/Vis (CH₃CN): λ_{\max} (ε) = 674 (26), 931 (54), 1023 nm (74 M⁻¹ cm⁻¹). C₅₀H₈₈Cl₂N₆Ni₂O₄S₂·CH₃CN·3H₂O (1089.69 + 41.05 + 54.06): calcd. C 52.71, H 8.25, N 8.28; found C 52.90, H 8.35, N 8.17.

[(L^{Et})Ni₂(OAc)]ClO₄ (9-ClO₄): To a solution of 7-ClO₄ (97.4 mg, 0.100 mmol) in methanol (25 mL) was added a solution of sodium acetate (16.4 mg, 0.200 mmol) in methanol (10 mL). After stirring for 2 h, solid LiClO₄·3H₂O (160 mg, 1.00 mmol) was added. The resulting pale-green precipitate was isolated by filtration, washed with methanol and dried in air. This material was recrystallized once from a mixed acetonitrile/ethanol solvent system. Yield: 73.5 mg (66%). M.p. 332 °C (decomp.). IR (KBr): $\tilde{\nu}$ = 3446 m, 2964 vs, 2900 s, 2359 vw, 1714 vw, 1589 s v_{asym}(OAc⁻), 1426 s v_{sym}(OAc⁻), 1383 s, 1326 w, 1313 w, 1248 w, 1231 m, 1202 vw, 1187 vw, 1151 m, 1101 vs v(ClO₄⁻), 987 w, 949 w, 928 vw, 907 w, 878 w, 783 m, 756 vw, 664 w, 623 s, 581 vw, 558 vw cm⁻¹. UV/Vis (CH₃CN): λ_{\max} (ε) = 345 (1596), 660 (29), 1180 nm (79 M⁻¹ cm⁻¹). C₄₆H₇₉ClN₆Ni₂O₆S₂ (1029.13): calcd. C 53.69, H 7.74, N 8.17, S 6.23; found C 53.34, H 7.72, N 8.10, S 6.08.

[(L^{Pr})Ni₂(μ-O₂CCH₃)]ClO₄ (10-ClO₄): This compound was prepared by the method detailed above for 9-ClO₄. Yield: 75.7 mg (68%). M.p. 319 °C (decomp.). IR (KBr): $\tilde{\nu}$ = 3445 m, 2963 vs, 2872 m, 1589 s v_{asym}(OAc⁻), 1457 m, 1428 m v_{sym}(OAc⁻), 1365 w, 1312 w, 1332 w, 1151 m, 1092 vs v_s(ClO₄⁻), 1061 vs, 937 w, 911 w, 876 w, 813 w, 755 w, 663 w, 626 m, 529 w cm⁻¹. UV/Vis (CH₃CN): λ_{\max} (ε) = 662 (29), 1183 nm (77 M⁻¹ cm⁻¹). C₅₂H₉₁ClN₆Ni₂N₆O₆S₂ (1113.29): calcd. C 56.10, H 8.24, N 7.55, S 5.76; found C 56.49, H 8.42, N 7.17, S 5.48.

[(L^{Et})Ni₂(μ-O₂COMe)]ClO₄ (11-ClO₄): To a solution of 7-ClO₄ (201 mg, 0.200 mmol) in a mixture of MeOH/H₂O (40 mL/ 5 mL) was added finely ground NaOH (20 mg, 0.50 mmol). The color of the reaction mixture turned from yellow to green. The reaction mixture was exposed to air and stirred at room temperature for 24 h. A solution of LiClO₄·3H₂O (1.00 g, 6.25 mmol) in methanol (2 mL) was then added. The green microcrystalline solid was isolated by filtration, washed with methanol and dried in vacuo. The yield was 182 mg (87%). M.p. 284–285 °C (decomp.). UV/Vis (CH₃CN): λ_{\max} (ε) = 670 (20), 1138 nm (49 M⁻¹ cm⁻¹). IR (KBr): $\tilde{\nu}$ = 3446 m, 2964 vs, 2901 m, 2357 vs, 1716 vw, 1638 vs v_{asym}(CH₃OCO₂⁻), 1450 vs, 1384 m, 1331 vs v_{sym}(CH₃OCO₂⁻), 1261 w, 1232 w, 1101 vs, v(ClO₄⁻), 987 vw, 950 vw, 908 vw, 979 vw, 785 s, 625 m, 581 vw, 560 vw cm⁻¹. UV/Vis (CH₃CN): λ_{\max} (ε) = 350 (2384), 668 (22), 1136 nm (84 M⁻¹ cm⁻¹). C₄₆H₇₉ClN₆Ni₂O₇S₂ (1045.13): calcd. C 52.86, H 7.62, N 8.04, S 6.14; found C 52.26, H 7.67, N 7.90, S 5.71.

[(L^{Et})Ni₂(μ-O₂COEt)]ClO₄ (12-ClO₄): The complex 11-ClO₄ (105 mg, 0.100 mmol) was dissolved in acetonitrile (20 mL). To the green solution was added ethanol (20 mL) and the reaction mixture was stirred at room temperature for 24 h. The solution was concentrated in vacuo to about 5 mL whereupon a pale-green precipitate formed. The precipitate was filtered, washed with a few milliliters of cold ethanol and dried in air. Yield: 75 mg (71%). M.p. 295 °C (decomp.). IR (KBr): $\tilde{\nu}$ = 3453 m, 2965 vs v(CH), 2900 s, 1638 vs v_{asym}(CH₃CH₂OCO₂⁻), 1449 vs, 1384 m, 1330 vw, 1316 vs v_{sym}(CH₃CH₂OCO₂⁻), 1248 w, 1231 m, 1187 w, 1151 m, 1101 vs v(ClO₄⁻), 1056 s, 987 vw, 949 vw, 908 vw, 878 vw, 806 w, 785 m, 756 w, 628 m, 582 vs, 560 vs cm⁻¹. UV/Vis (CH₃CN): λ_{\max} (ε) = 350 (2550), 668 (28), 1140 nm (79 M⁻¹ cm⁻¹). C₄₇H₈₁ClN₆Ni₂O₇S₂ (1059.15): calcd. C 53.30, H 7.71, N 7.93, S 6.05; found C 52.48, H 7.65, N 7.76, S 5.85. The tetraphenylborate salt, [(L^{Et})Ni₂(μ-O₂COEt)]BPh₄ (12-BPh₄), was prepared by adding NaBPh₄ (342 mg, 1.00 mmol) to a solution of [(L^{Et})Ni₂(μ-O₂COEt)]ClO₄ (106 mg, 0.100 mmol) in methanol (40 mL). The pale-green microcrystalline solid was isolated by filtration, washed with ethanol and dried in air. Yield: 116 mg (91%). M.p. 293–294 °C (decomp.). IR (KBr): $\tilde{\nu}$ = 3442 s v(OH), 3056 s v(ArH), 2968 vs v(CH), 2903 s v(CH), 1634 vs v_{asym}(CH₃CH₂OCO₂⁻), 1579 m, 1478 s, 1463 s, 1427 m, 1397 m, 1373 m, 1316 vs v_{sym}(CH₃CH₂OCO₂⁻), 1261 w, 1231 w, 1185 m, 1154 m, 1102 s, 1056 s, 948 vw, 909 vw, 879 vw, 854 vw, 803 w, 744 vs v(BPh₄⁻), 715 vs v(BPh₄⁻), 628 w, 612 w, 560 w cm⁻¹. UV/Vis (CH₃CN): λ_{\max} (ε) = 668 (27), 1140 nm (70 M⁻¹ cm⁻¹). The tetraphenylborate salt was additionally characterized by X-ray crystal structure analysis.

[(L^{Et})Ni₂](ClO₄)₃ (13-(ClO₄)₃): To a solution of 7-ClO₄ (101 mg, 0.100 mmol) in MeOH (30 mL) was added Pb(ClO₄)₂ (40.6 mg, 0.100 mmol). The resulting dark green solution was stored at room temperature for 12 h during which a few crystals of the title compound precipitated as dark green crystals. Yield: 16 mg (13%). The ¹H NMR spectra obtained for the trication are broad with chemical shifts ranging from δ = +200 to –50 ppm and almost completely collapse into the base line, indicative of a paramagnetic species. UV/Vis (CH₃CN): λ_{\max} (ε) = 574 (850), 1016 nm (50 M⁻¹ cm⁻¹). This compound was additionally characterized by X-ray crystal structure analysis.

[(L^{Et})Zn₂(OAc)]ClO₄ (14-ClO₄): To a suspension of H₂L^{Et}·6HCl (974 mg, 1.00 mmol) in methanol (50 mL) was added a solution of Zn(OAc)₂·2H₂O (439 mg, 2.00 mmol) in methanol (5 mL). A solution of triethylamine (810 mg, 8.00 mmol) in methanol (1 mL) was added and the resulting clear solution was stirred at room temperature for 12 h. Solid LiClO₄·3H₂O (1.60 g, 10.0 mmol) was then

added. The resulting colorless precipitate was isolated by filtration, washed with methanol and dried in air. Yield: 830 mg (80%). M.p. 282–284 °C (decomp.). IR (KBr): $\tilde{\nu}$ = 3442 m, 2964 vs, 2899 s, 1585 s $\nu_{\text{asym}}(\text{OAc}^-)$, 1464 s, 1442 vw $\nu_{\text{sym}}(\text{OAc}^-)$, 1385 m, 1329 w, 1252 w, 1230 w, 1149 m, 1100 vs $\nu(\text{ClO}_4^-)$, 1056 vs, 947 vw, 906 w, 884 w, 782 w, 656 vw, 625 s, 578 vw, 553 vw cm^{-1} . ^1H NMR (300 MHz, CD_3CN , 25 °C, TMS): δ = 7.13 (s, 4 H, ArH), 4.12 (d, 2J = 12.0 Hz, 4 H, ArCH₂), 3.21 (d, 2J = 12.0 Hz, 4 H, ArCH₂), 3.60–2.60 (m, 28 H, NCH₂CH₂ + NCH₂), 1.25 (t, 3J = 7.0 Hz, 6 H, NCH₂CH₃), 1.23 [s, 18 H, C(CH₃)₃], 1.16 (t, 3J = 7.0 Hz, 12 H, NCH₂CH₃), 0.83 (s, 3 H, CO₂CH₃) ppm. $^{13}\text{C}\{^1\text{H}\}$ NMR (75 MHz, CD_3CN , 25 °C, TMS): δ = 174.74 (C=O), 145.96 (C), 143.85 (C), 135.65 (C), 128.30 (CH), 54.96, 54.17, 53.47, 53.16, 47.53 (all CH₂), 34.53 [C(CH₃)₃], 31.55 [C(CH₃)], 23.12 (COCH₃), 6.87 (ArCH₂NCH₂CH₃), 4.58 (NCH₂CH₃). The tetraphenylborate salt, [(L^{Et})Zn₂(OAc)]BPh₄ (**14**·BPh₄), was prepared by adding NaBPh₄ (342 mg, 1.00 mmol) to a solution of [(L^{Et})Zn₂(OAc)]ClO₄ (104 mg, 0.100 mmol) in methanol (50 mL). The colorless, microcrystalline solid was isolated by filtration, washed with methanol and dried in air. Yield: 115 mg (91%). M.p. 246–248 °C (decomp.). IR (KBr): $\tilde{\nu}$ = 1582 s $\nu_{\text{asym}}(\text{OAc}^-)$, 1440 s $\nu_{\text{sym}}(\text{OAc}^-)$, 703, 732 $\nu(\text{BPh}_4^-)$ cm^{-1} . C₇₀H₉₉BN₆O₂S₂Zn₂ (1262.30): calcd. C 66.60, H 7.91, N 6.66, S 5.08; found C 66.89, H 7.85, N 6.45, S 4.84. Compound **14**·ClO₄ was also characterized by X-ray crystal structure analysis.

[(L^{Et})Co₂(μ-Cl)]ClO₄ (**17**·ClO₄): To a suspension of H₂L^{Et}·6HCl (974 mg, 1.00 mmol) in methanol (40 mL) was added a solution of CoCl₂·6H₂O (476 mg, 2.00 mmol) in methanol (2 mL). A solution of Et₃N (810 mg, 8.00 mmol) in methanol (2 mL) was then added to give a dark red solution. After stirring at room temperature for 3 d, the product was precipitated by the addition of solid LiClO₄·3H₂O (2.50 g, 15.6 mmol). The red microcrystalline solid was isolated by filtration, washed with 5 mL of cold ethanol and 5 mL of ether, and dried in vacuo. This material was recrystallized once from a few milliliters of acetonitrile. Yield: 765 mg (76%). M.p. 313 °C (decomp.). IR (KBr): $\tilde{\nu}$ = 3443 s, 2963 vs, 2867 s, 2354 vw, 1730 vw, 1696 vw, 1634 w, 1556 vw, 1540 vw, 1518 vw, 1478 s, 1463 s, 1382 m, 1327 w, 1278 vw, 1251 w, 1231 w, 1202 vw, 1159 m, 1099 vs $\nu(\text{ClO}_4^-)$, 987 vw, 956 vw, 913 vw, 884 w, 803 vw,

776 m, 732 vw, 674 vw, 624 m cm^{-1} . UV/Vis (CH_3CN): λ_{max} (ϵ) = 342 (2401), 470 (602), 548 sh (174), 578 (161), 1280 nm (28 $\text{M}^{-1} \text{cm}^{-1}$). C₄₄H₇₆Cl₂Co₂N₆O₄S₂·H₂O (1006.01 + 18.02): calcd. C 51.61, H 7.68, N 8.21, S 6.26; found C 51.20, H 7.39, N 8.37, S 6.25.

[(L^{Et})Co₂(OAc)]ClO₄ (**18**·ClO₄): A solution of sodium acetate (41 mg, 0.50 mmol) in methanol (5 mL) was added to a solution of [(L^{Et})Co₂(μ-Cl)]ClO₄ (202 mg, 0.200 mmol) in methanol (40 mL). The mixture was stirred for 1 h, during which the color of the solution turned to light brown. A solution of LiClO₄·3H₂O (320 mg, 2.00 mmol) in methanol (2 mL) was added. The resulting light brown solid was isolated by filtration, washed with cold methanol and dried in air. This compound was recrystallized once from a mixed acetonitrile/ethanol (1:1) solvent system. Yield: 152 mg (74%). M.p. 337–338 °C (decomp.). IR (KBr): $\tilde{\nu}$ = 3442 m, 2964 vs, 2898 s, 1588 vs $\nu_{\text{asym}}(\text{OAc}^-)$, 1440 vs $\nu_{\text{sym}}(\text{OAc}^-)$, 1384 s, 1361 m, 1326 w, 1314 w, 1249 w, 1230 s, 1187 vw, 1152 m, 1100 vs $\nu(\text{ClO}_4^-)$, 1055 s, 986 w, 948 w, 928 w, 906 w, 880 w, 783 m, 755 vw, 653 w, 626 s cm^{-1} . UV/Vis (CH_3CN): λ_{max} (ϵ) = 338 (2203), 440 (610), 528 (204), 1288 nm (44 $\text{M}^{-1} \text{cm}^{-1}$). CV (CH_3CN , 295 K, 0.1 M *n*Bu₄NPF₆, ν = 100 mV/s; *E* (vs. SCE): $E^1_{1/2}$ = +0.27 V (ΔE_p = 0.126 V), $E^2_{1/2}$ = +0.64 V (ΔE_p = 0.131 V). The tetraphenylborate salt, [(L^{Et})Co₂(OAc)] BPh₄ (**18**·BPh₄), was prepared by adding NaBPh₄ (342 mg, 1.00 mmol) to a solution of [(L^{Et})Co₂(μ-O₂CCH₃)] ClO₄ (103 mg, 0.100 mmol) in methanol (50 mL). The light brown microcrystalline solid was isolated by filtration, washed with methanol and dried in air. Yield: 113 mg (90%). M.p. 318–319 °C (decomp.). IR (KBr): $\tilde{\nu}$ = 3437 m, 3055 s $\nu(\text{Ar})$, 2968 vs, 2866 s, 1582 vs $\nu_{\text{asym}}(\text{OAc}^-)$, 1440 vs $\nu_{\text{sym}}(\text{OAc}^-)$, 1383 m, 1326 w, 1310 w, 1248 w, 1231 w, 1185 vw, 1154 w, 1100 m, 1057 vs, 1033 w, 987 vw, 951 vw, 909 w, 882 w, 844 vw, 780 m, 732 s $\nu(\text{BPh}_4^-)$, 704 vs $\nu(\text{BPh}_4^-)$, 653 vw, 626 w, 612 m, 579 vw, 557 vw cm^{-1} . UV/Vis (CH_3CN): λ_{max} (ϵ) = 442 (597), 528 (196), 1294 nm (43 $\text{M}^{-1} \text{cm}^{-1}$). C₇₀H₉₉BCo₂N₆O₂S₂ (1249.38): calcd. C 67.29, H 7.99, N 6.73, S 5.13; found C 66.96, H 7.73, N 7.03, S 4.95.

Crystal Structure Determinations: Single crystals of [(L^{Pr})Ni₂(OAc)]·ClO₄·MeOH (**10**·ClO₄·MeOH), [(HL^{Et})Ni₂]·3ClO₄·3MeOH·H₂O (**13**·3ClO₄·3MeOH·H₂O) and [(L^{Et})Zn₂(OAc)]·ClO₄·MeOH

Table 4. Crystallographic data for complexes **10**, **12**, **13**, **14**, and **18**.

Compound	10 ·ClO ₄ ·MeOH	12 ·BPh ₄ ·MeCN·EtOH	13 ·(ClO ₄) ₃ ·3MeOH·H ₂ O	14 ·ClO ₄ ·2MeOH	18 ·BPh ₄ ·EtOH
Empirical formula	C ₅₃ H ₉₅ ClN ₆ Ni ₂ O ₇ S ₂	C ₇₅ H ₁₁₀ BN ₇ Ni ₂ O ₄ S ₂	C ₄₇ H ₉₁ Cl ₃ N ₆ Ni ₂ O ₁₆ S ₂	C ₄₇ H ₈₃ ClN ₆ O ₇ S ₂ Zn ₂	C ₇₂ H ₁₀₂ BCo ₂ N ₇ O ₂ S ₂
<i>M_r</i> [g/mol]	1145.34	1366.05	1284.15	1074.50	1290.40
Space group	<i>P</i> 2 ₁ / <i>n</i>	<i>P</i> 2 ₁ / <i>n</i>	<i>P</i> 1̄	<i>C</i> 2/ <i>c</i>	<i>P</i> 2 ₁ / <i>c</i>
<i>a</i> [Å]	14.810(3)	16.346(3)	13.551(3)	16.385(3)	15.734(3)
<i>b</i> [Å]	20.793(4)	29.155(6)	14.076(3)	29.778(6)	26.293(5)
<i>c</i> [Å]	21.376(4)	16.945(3)	16.661(3)	13.310(3)	18.319(4)
α [°]	90	90	77.77(3)	90	90.00
β [°]	108.78(3)	114.22(3)	89.92(3)	123.56(3)	112.14(3)
γ [°]	90	90	75.24(3)	90	90.00
<i>V</i> [Å ³]	6232(2)	7365(2)	2999(1)	5412(2)	7019.7(24)
<i>Z</i>	4	4	2	4	4
<i>d</i> _{calcd.} [g/cm ³]	1.221	1.232	1.421	1.358	1.221
Crystal size [mm]	0.45 × 0.30 × 0.30	0.30 × 0.15 × 0.15	0.20 × 0.20 × 0.20	0.35 × 0.26 × 0.18	0.30 × 0.20 × 0.20
$\mu(\text{Mo-K}\alpha)$ [mm ⁻¹]	0.764	0.620	0.899	1.064	0.580
2 θ limits [°]	3.50–56.76	2.80–56.66	3.06–56.62	4.58–56.70	2.80–56.62
Measured reflections	39885	46840	27268	17437	44376
Independent reflections	15063	17670	14028	6519	16817
Observed reflections ^[a]	3609	8078	7533	2860	6415
Number of parameters	604	791	697	341	748
<i>R</i> ^[b] (<i>R</i> ₁ all data)	0.0774 (0.2867)	0.0779 (0.1497)	0.0540 (0.1117)	0.0434 (0.1373)	0.0717 (0.1676)
<i>wR</i> ^[c] (<i>wR</i> ₂ all data)	0.1928 (0.2636)	0.1966 (0.2369)	0.1229 (0.1529)	0.0858 (0.1133)	0.1805 (0.2100)
Max/min peaks [e/Å ³]	1.237/−0.653	1.129/−1.888	0.770/−0.742	0.386/−0.523	1.583/−0.672

[a] Observation criterion: $I > 2\sigma(I)$. [b] $R_1 = \sum ||F_o| - |F_c|| / \sum |F_o|$. [c] $wR_2 = \{\sum [w(F_o^2 - F_c^2)^2] / \sum [w(F_o^2)]\}^{1/2}$.

(14·ClO₄·MeOH) were taken directly from the reaction mixtures. Crystals of [(L^{Et})Ni₂(O₂COEt)]BPh₄·MeCN·EtOH (12·BPh₄·MeCN·EtOH) and [(L^{Et})Co₂(OAc)]BPh₄·EtOH (18·BPh₄·EtOH) were grown by recrystallization from an acetonitrile/ethanol (1:1) mixed solvent system. The crystals were mounted on glass fibers using perfluoropolyether oil. Intensity data were collected at 210(2) K, using a Bruker SMART CCD diffractometer. Graphite-monochromated Mo-K_α radiation (λ = 0.71073 Å) was used throughout. Crystallographic data of the compounds are listed in Table 4. The data were processed with SAINT^[30] and corrected for absorption using SADABS^[31] [transmission factors: 1.00–0.92 (10, 13), 1.00–0.89 (12, 18), 1.00–0.87 (14)]. The structures were solved by using the program SHELXS-86.^[32] Refinements were carried out with the program SHELXL-97.^[33] PLATON was used to search for higher symmetry.^[34] ORTEP-3 was used for the artwork of the structures.^[35] Where appropriate, all non-hydrogen atoms were refined anisotropically. Hydrogen atoms were assigned to idealized positions and given isotropic thermal parameters 1.2 times (1.5 times for CH₃ groups) the thermal parameter of the atoms to which they were attached. In the crystal structure of 10·ClO₄·MeOH a propyl group, a *tert*-butyl group and a ClO₄[−] ion were found to be disordered over two positions. The site occupancies of the respective positions were refined as follows: C(18a)–C(20a)/C(18b)–C(20b) 0.50(2)/0.50(2); C(48a)–C(50a)/C(48b)–C(50b): 0.55(2)/0.45(2); O(3a)–O(6a)/O(3b)–O(6b) 0.70(1)/0.30(1). The C and O atoms of the disordered groups and the solvate molecules were refined isotropically. In the crystal structure of 12·BPh₄·MeCN·EtOH the C, N, and O atoms of the solvate molecules were refined isotropically. In the crystal structure of 13·3ClO₄·3MeOH·H₂O one *tert*-butyl group and two methanol molecules of solvent of crystallization were found to be disordered over two positions [C(42a)–C(44a)/C(42b)–C(44b) 0.53(2)/0.47(2); O(14)–C(45a)/O(14)–C(45b) 0.57(2)/0.43(2), and O(15a)–C(46a)/O(15b)–C(46b) 0.47(2)/0.53(2)]. In the crystal structure of 14·ClO₄·MeOH a *tert*-butyl group and the counteranion were found to be disordered over two positions [C(20a)–C(22a)/C(20b)–C(22b) 0.47(2)/0.53(2); O(2a), O(3a)/O(2b), O(3b) 0.71(2)/0.29(2)]. In the crystal structure of 18·BPh₄·EtOH one *tert*-butyl group was found to be disordered over two positions at site occupancies of 0.53(2) [C(42a)–C(44a)] and of 0.47(2) [C(42b)–C(44b)]. The C and O atoms of the solvate molecule and the disordered groups were refined isotropically. CCDC-259281 (10), -259282 (12), -259283 (13), -259284 (14) and -259285 (18) contains the supplementary crystallographic data for this paper. These data can be obtained free of charge from The Cambridge Crystallographic Data Centre via www.ccdc.cam.ac.uk/data_request/cif.

Acknowledgments

We are particularly grateful to Prof. Dr. H. Vahrenkamp for providing facilities for NMR and X-ray crystallographic measurements. Financial support of this work from the Deutsche Forschungsgemeinschaft (Priority programme “Sekundäre Wechselwirkungen”, KE 585/3-1,2) is gratefully acknowledged.

- [1] J. W. Canary, B. C. Gibb, *Prog. Inorg. Chem.* **1997**, *45*, 1–83.
- [2] a) B. R. Cameron, S. J. Loeb, G. P. A. Yap, *Inorg. Chem.* **1997**, *36*, 5498–5504; b) B. S. Hammes, D. Ramos-Maldonado, G. P. A. Yap, L. Liable-Sands, A. L. Rheingold, V. G. Young, Jr., A. S. Borovik, *Inorg. Chem.* **1997**, *36*, 3210–3211.
- [3] a) S. Blanchard, L. Le Clainche, M.-N. Rager, B. Chansou, J.-P. Tuchagues, A. F. Duprat, Y. Le Mest, O. Reinaud, *Angew. Chem.* **1998**, *110*, 2861–2864; *Angew. Chem. Int. Ed. Engl.* **1998**,

- 37, 2732–2735; b) Y. Rondelez, G. Bertho, O. Reinaud, *Angew. Chem.* **2002**, *114*, 1086–1088; *Angew. Chem. Int. Ed.* **2002**, *41*, 1044–1046.
- [4] a) M. T. Reetz, S. R. Waldvogel, *Angew. Chem.* **1997**, *109*, 870–873; *Angew. Chem. Int. Ed. Engl.* **1997**, *36*, 865–867; b) M. T. Reetz, *Catal. Today* **1998**, *42*, 399.
- [5] For reviews of cyclodextrins, see: *Chem. Rev.* **1998**, *98*, 1741–2076 (special issue).
- [6] a) N. Kitajima, W. B. Tolman, *Prog. Inorg. Chem.* **1995**, *43*, 419–531; b) S. Trofimenko, *Scorpionates: The Coordination Chemistry of Polypyrazolylborate Ligands*; Imperial College Press, London, U. K., **1999**; c) H. Vahrenkamp, *Acc. Chem. Res.* **1999**, *32*, 589–596.
- [7] P. Chaudhuri, K. Wieghardt, *Prog. Inorg. Chem.* **1987**, *35*, 329–436.
- [8] N. H. Pilkington, R. Robson, *Aust. J. Chem.* **1970**, *23*, 2225–2236.
- [9] a) M. H. Klingele, G. Steinfeld, B. Kersting, *Z. Naturforsch.* **2001**, *56b*, 901–907; b) B. Kersting, G. Steinfeld, *Inorg. Chem.* **2002**, *41*, 1140–1150; c) B. Kersting, *Z. Allg. Anorg. Chem.* **2004**, *630*, 765–780.
- [10] B. Kersting, G. Steinfeld, *Chem. Commun.* **2001**, 1376–1377.
- [11] B. Kersting, *Angew. Chem.* **2001**, *113*, 4109–4112; *Angew. Chem. Int. Ed.* **2001**, *40*, 3987–3990.
- [12] G. Steinfeld, V. Lozan, B. Kersting, *Angew. Chem.* **2003**, *115*, 2363–2365; *Angew. Chem. Int. Ed.* **2003**, *42*, 2261–2263.
- [13] K. Wieghardt, P. Chaudhuri, B. Nuber, J. Weiss, *Inorg. Chem.* **1982**, *21*, 3086–90.
- [14] N. W. Alcock, A. C. Benninston, S. J. Grant, H. A. A. Omar, P. Moore, *J. Chem. Soc. Chem. Commun.* **1991**, 1573–1575.
- [15] B. Kersting, G. Steinfeld, T. Fritz, J. Hausmann, *Eur. J. Inorg. Chem.* **1999**, 2167–2172.
- [16] a) M. H. Klingele, G. Steinfeld, B. Kersting, *Z. Naturforsch.* **2001**, *56b*, 901–907; b) G. Siedle, B. Kersting, *Z. Anorg. Allg. Chem.* **2003**, *629*, 2083–2090.
- [17] Complex 5·ClO₄ is also readily dehalogenated with Pb(ClO₄)₂. However, the resulting [(HL^{Me})Ni₂]³⁺ intermediate reacts instantaneously with a ClO₄[−] anion to give the perchlorate complex [(L^{Me})Ni₂(μ_{1,3}-ClO₄)]⁺. The structure of this compound will be reported elsewhere.
- [18] B. Kersting, G. Steinfeld, *Inorg. Chem.* **2002**, *41*, 1140–1150.
- [19] For a complete list of the IR absorptions, see Exp. Sect.
- [20] K. Nakamoto, *Infrared and Raman Spectra of Inorganic and Coordination Compounds*, 5th ed., Wiley-VCH, New York, **1997**.
- [21] a) I. Murase, S. Ueno, S. Kida, *Bull. Chem. Soc. Jpn.* **1983**, *56*, 2748–2751; b) G. A. Lawrance, M. Maeder, T. M. Manning, M. A. O’Leary, B. W. Skelton, A. H. White, *J. Chem. Soc. Dalton Trans.* **1990**, 2491–2495.
- [22] M. D. Santana, G. Garcia, J. Perez, E. Molins, G. Lopez, *Inorg. Chem.* **2001**, *40*, 5701–5703.
- [23] The high-spin d⁷ configuration for the present cobalt(II) complexes is also supported by temperature-dependent magnetic susceptibility measurements. The results of these studies will be reported in due course.
- [24] J. Hausmann, S. Käss, S. Klod, E. Kleinpeter, B. Kersting, *Eur. J. Inorg. Chem.* **2004**, 4402–4411.
- [25] D. A. House, *Comprehensive Coordination Chemistry* (Eds.: G. Wilkinson, R. D. Gillard, J. A. McCleverty), Pergamon Press, Oxford, **1996**, vol. 2, p. 23–72.
- [26] a) D. K. Mills, J. H. Reibenspies, M. Y. Darensbourg, *Inorg. Chem.* **1990**, *29*, 4364–4366; b) D. K. Mills, Y. M. Hsiao, P. J. Farmer, E. V. Atnip, J. H. Reibenspies, M. Y. Darensbourg, *J. Am. Chem. Soc.* **1991**, *113*, 1421–1423; c) R. M. Buonomo, I. Font, M. J. Maguire, J. H. Reibenspies, T. Tuntulani, M. J. Darensbourg, *J. Am. Chem. Soc.* **1995**, *117*, 963–973.
- [27] C. A. Grapperhaus, M. J. Maguire, T. Tuntulani, M. Y. Darensbourg, *Inorg. Chem.* **1997**, *36*, 1860–1866.
- [28] a) N. Baidya, M. M. Olmstead, P. K. Mascharak, *Inorg. Chem.* **1991**, *30*, 929–937; b) N. Baidya, M. M. Olmstead, J. P. White-

- head, C. Bagyinka, M. J. Maroney, P. K. Mascharak, *Inorg. Chem.* **1992**, *31*, 3612–3619.
- [29] C. A. Marganian, H. Vazir, N. Baidya, M. M. Olmstead, P. K. Mascharak, *J. Am. Chem. Soc.* **1995**, *117*, 1584–1594.
- [30] *SAINT+*, V6.02, Bruker AXS, Madison, WI, **1999**.
- [31] *SADABS*, An empirical absorption correction program, part of SAINTPlus NT, version 5.10, Bruker AXS, Madison, WI, **1998**.
- [32] G. M. Sheldrick, *Acta Crystallogr., Sect. A* **1990**, *46*, 467–473.
- [33] G. M. Sheldrick, *SHELXL-97*, Computer program for crystal structure refinement, University of Göttingen, Göttingen, Germany, **1997**.
- [34] A. L. Spek, *PLATON – A Multipurpose Crystallographic Tool*, Utrecht University, Utrecht, The Netherlands, **2000**.
- [35] L. J. Farrugia, *J. Appl. Crystallogr.* **1997**, *30*, 565–568..

Received January 10, 2005